Spring 5-13-2017

The Limiting Effect of Cytoplasmic Volume on Microtubule Dynamics

Jacob Zumo
jzumo@uwyo.edu

The Limiting Effect of Cytoplasmic Volume on Microtubule Dynamics

Jacob Zumo
Spring 2017
B.S. in Molecular Biology and Microbiology
Honors Program
Principle Investigator: Dr. Jesse Gatlin, Molecular Biology
University of Wyoming

Abstract:

Mitotic spindles play a key role in cellular division. These structures, which are composed of dynamic filaments called microtubules, are responsible for separation and segregation of chromosomes during mitosis. Spindles must be the correct shape and size to insure fidelity of this process, however, their formation and assembly are still not entirely understood. For example, the mechanisms that govern spindle shape and determine individual spindle size for a given cell type are still unknown. Based on evidence from recent studies of spindle scaling, in which spindle size effectively scaled with cell size, we hypothesize that within small cytoplasmic volumes, spindle building blocks become limiting and thereby limit spindle size. This hypothesis predicts that microtubule dynamics within the spindle will be adversely affected by changes in cytoplasmic volume. By combining cell-free cytoplasmic extracts, microfluidics, and confocal microscopy, we hope to measure changes in microtubule dynamics to elucidate the relationship between cell volume and spindle size within the cell.

Background:

Cellular division is a topic most individuals can conceptualize. For a cell to faithfully replicate and divide, it must ensure that the new daughter cells are given equal amounts of the same genetic material that was produced during DNA replication. Mitotic spindles play a key role in cellular division. They are responsible for the segregation of chromosomes into daughter cells during mitosis. These spindles are composed of microtubules, filamentous polymers made up of heterodimeric protein subunits called tubulin (Feit et al, 1971). Microtubules are inherently dynamic filaments in the sense that they must grow and shorten to function, e.g. to bind to and

separate the chromosomes during mitosis. The dynamics of microtubules are determined by several different parameters including growth rate, shrinkage rate, and the frequencies of transitions between the two states (Akhmanova and Steinmetz, 2015). It makes sense that these dynamics might affect spindle size. Indeed, the rate at which microtubules grow, the tubulin mass that has been incorporated into the microtubules, and the average length of the microtubules all affect spindle size. For example, within *Xenopus laevis*, a balance of mass is required between the rate of tubulin entering spindle and that of tubulin leaving spindle assembly (Reber et al, 2013).

In order to maintain homeostasis, every living cell must be able to regulate the size of its internal parts regardless of its own size. The geometric relationship is termed scaling and comes in two forms: isometric scaling and allometric scaling. When two objects that are geometrically similar, for example a small equilateral triangle and a larger equilateral triangle, they are said to exhibit isometry. Isometric scaling would mean that the relationships between volume and surface area would remain constant between different sizes of cells because the cells are geometrically similar. Allometry refers to a change in shape in response to a change in size. This means that allometric scaling would result in not only a change in size, but shape. Scaling occurs at the extreme of cell sizes - bacteria as small as 1µm in diameter and *X. laevis* blastomeres, which can be up to 1.2mm in diameter (some 1000 times larger) both must scale their replication machinery as a means for survival. In eukaryotes, failure of chromosome separation can lead to aneuploidy, which can lead to problems like Down's Syndrome and cancer (Fang and Zhang, 2011). This scaling challenge is essential for normal development. Spindles must be in the correct size and

shape in order effectively ensure fidelity of this process. Dynamics of microtubules affect spindle size and shape (Dumont and Mitchison, 2009). It is generally observed that, up until a point, as cell diameter increases, so does spindle length (Wühr et al, 2008). This is true up until a certain point where relationship plateaus (Wühr et al, 2008). This suggests that to the relationship between cell size and spindle size could be regulated by limiting components, changes in cytoplasmic composition that accompany developmental progression, or negative feedback induced by sterically constraining spindles in small volumes.

It is known that enzymes are involved in the regulation of spindle size however this process is not entirely understood (Reber et al, 2013; Petry, 2016). Currently, a "limiting component" model is generally accepted (Good et al 2013, Hazel et al 2013). This mode posits that for a system of microtubules (e.g. a spindle) is built in small cellular environment, the cytoplasmic concentrations of spindle components and enzymes required to assemble them will be more greatly affected than in a larger cell building the same structure. For example, the enzyme XMAP215, which is part of a family of proteins that promotes microtubule growth, can directly catalyze the addition up to 25 tubulin dimers to the growing end of the molecule (Brouhard et al, 2008). This leads to the general question of not only how does cell size determine spindle size, but also the rate at which spindles are formed. We hypothesized that if spindle assembly occurs in a larger cell volume, then these spindles will be formed at a faster rate than cells of a smaller volume because they would be able to maintain a saturating number of enzyme molecules per growing microtubule end. In a small cellular volume, the relative starting concentration of that enzyme might still be the same, however the number of enzyme molecules per microtubule growing end

would be sub-saturating, resulting in a slower rate of microtubule assembly. Cells of different volumes would still have the same concentrations of this enzyme. However, once microtubules begin to assemble, and the enzymes that bind them are effectively pulled out of solution to add tubulin subunits to growing ends, lowering the degree of saturation of this enzyme on those growing ends (Reber et al, 2013; Brouhard et al, 2008).

X. laevis egg extracts have a long and extensive history for use as model cell-free systems. In 1985, Lohka and Maller demonstrated that nuclear envelope breakdown, chromosome condensation, and spindle assembly could all be studied *iv vitro* using extracts of amphibian eggs (Lohka and Maller, 1985). This system has been used to research several fundamental biological processes ranging from analyzing the effect cigarette smoke has on the inhibition of CFTR expression, to studying stability of the DNA replication fork (Moran et al, 2014; Hashimoto and Costanzo, 2011).

X. laevis frogs were injected with hormones so they could lay eggs (as described in Desai et al, 1999). Once the eggs were harvested, they were washed with buffer and de-jellied, and packed into a test tube to remove any excess buffer. A crushing spin produced a stratified and fractionated extract from which the cytoplasmic layer was collected. This cytoplasmic extract is what we used to visualize and analyze microtubule growth. There are several advantages to using this cell-free system. It allows for easy controlling of *in vitro* processes, with protein biosynthesis being especially important for this experiment. Additionally, the absence of a cellular membrane

usually allows for a faster reaction then microbial systems with cellular membranes (Zhu et al, 2013; Martín del Campo et al, 2013).

Droplet microfluidics allow us to perform laboratory operations on very small scales (Mashaghi, et al, 2016). We could take our cytoplasmic extract and emulsify it with a surfactant and oil phase. As the name implies, this is done at a microscopic scale, at a size which we can control. Filling a single device can provide thousands of individual extract droplets. This provides us with flexibility to search under the microscope for the droplets with specific conditions we are interested in studying.

We utilized this system to test our prediction that larger cellular volumes will result in a faster rate of microtubule growth and ultimately larger spindles. By using cell-free cytoplasmic extracts, we did not have to rely on genetic in vivo control of cell size. By inserting fluorescently labeled proteins we could visualize and analyze microtubule growth rates using confocal microscopy. Using droplet microfluidics, we could control the size of the extract droplets in which microtubule structures were assembled, which is analogous to controlling the volume of the cell.

Materials and Methods:

Extract and protein solution preparation- 500µL of cytoplasmic extract from the eggs of *X. laevis* was prepared according to Desai and kept on ice (Desai et al, 1999). A genetically encoded microtubule, consisting of the microtubule binding domain of the Tau protein (Elie et al, 2015) was fused to mCherry (mCherry-Tau), expressed and purified in E. coli, and stored at a stock

concentration of 180µM (working concentration was ~1 µM; Mooney et al, in press), was used to visualize microtubules emanating from artificial microtubule organizing centers (aMTOCs; Field et al, 2017; Tsai and Zheng, 2005) used at a concentration to achieve 0 to 1 aMTOCs per extract droplet. End-binding protein 1 fused to GFP (EB1:56µM) was added to the mixture at a 1:100 dilution. Both 100x calcium at 40mM and 100x cycloheximide at 35mM were diluted to a a 1:100 working concentration. This extract mixture was kept on ice until droplets could be made.

Assembly of droplets- A microfluidic-based platform for confining spindle assembly to desired droplet size according to Hazel et al, 2013. Picosurf surfactant was used to suspend the extract mixture, and responsible for forming the extract into droplets. Different sized droplet devices were used to allow for small and large droplet sizes and volumes. 1mL NormJect syringes were used to inject the extract mixture and the surfactant at precise volumes utilizing syringe pumps (Cetoni Corp). The syringes and droplet devices were kept on ice until ready for use. The devices were filled in a room at 0°C to limit the temperature-sensitive assembly until ready to be viewed on the confocal microscope. The mixing of the extract and surfactant at a T-junction within the device allowed for the suspension of extract to become stabilized droplets of relatively similar size. After filling the device with droplets, the tubes were removed and the holes were covered with nail polish to act as a seal. The device was placed on ice prior to viewing under the confocal microscope. 600µL of extract allowed two to three devices to be filled at once. This experiment utilized a 63µL device, and a 113µL device to ensure droplets of different sizes and volumes could be analyzed.

Imagining spindle formation- Imaging of the spindle assembly was completed on a confocal microscope at 60x magnification under oil immersion. Time-lapses were completed at 2.5 second intervals for three minutes. EB1 protein tracking was done with the mTrackJ plugin on the image analysis software Fiji.

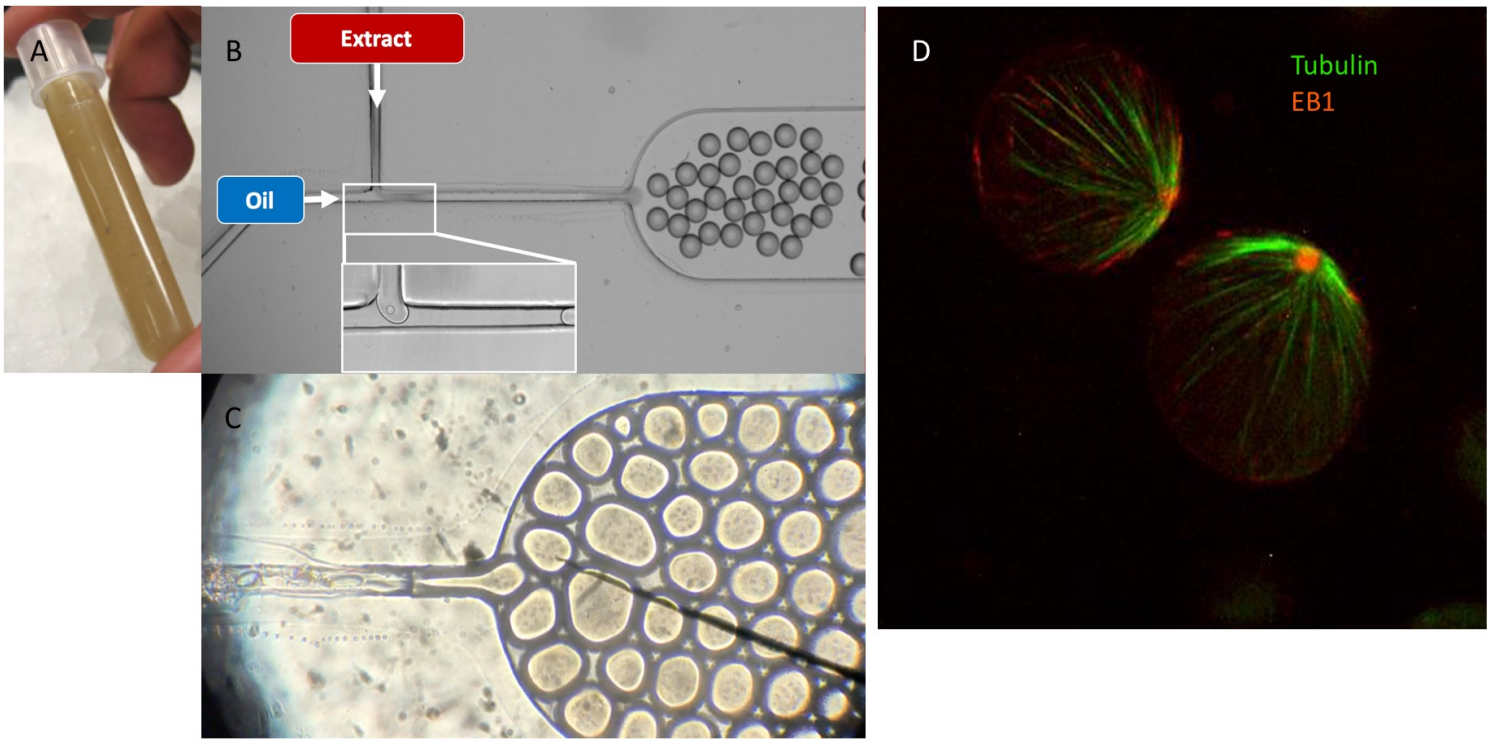

Figure1: **A,** the processed egg extract in which aMTOCs, mCherry-Tau, and EB1-GFP were added. **B,** a diagram of the T-junction devices used to create the droplets (Gatlin, 2017). An oil phase containing surfactant was pumped into the device through one inlet, while the extract and protein solution entered from another. After meeting at the T-junction, the surfactant emulsified the extract into droplets. **C** shows the droplets being formed as viewed from a microscope under the 20x objective lens. **D** demonstrates the relationship of EB1 and tubulin using images captured by the confocal microscope. EB1 protein (pseudocolored red) attached to the growing ends of the microtubules (pseudocolored green). These fluorescently tagged proteins were tracked to analyze microtubule assembly velocity.

Data:

Microtubule growth rates from individual aMTOCs were measured in two droplets of different sizes (**Fig 2**). The first droplet had a diameter of 62µm, and the second droplet had a diameter of 86µm. Manual tracking was used to measure the velocities of twenty growing microtubule ends using the MtrackJ plugin in Fiji (NIH). The mean velocity of all of the comets' average velcocities was determined for each droplet to asses average microtubule assembly velocity for each droplet

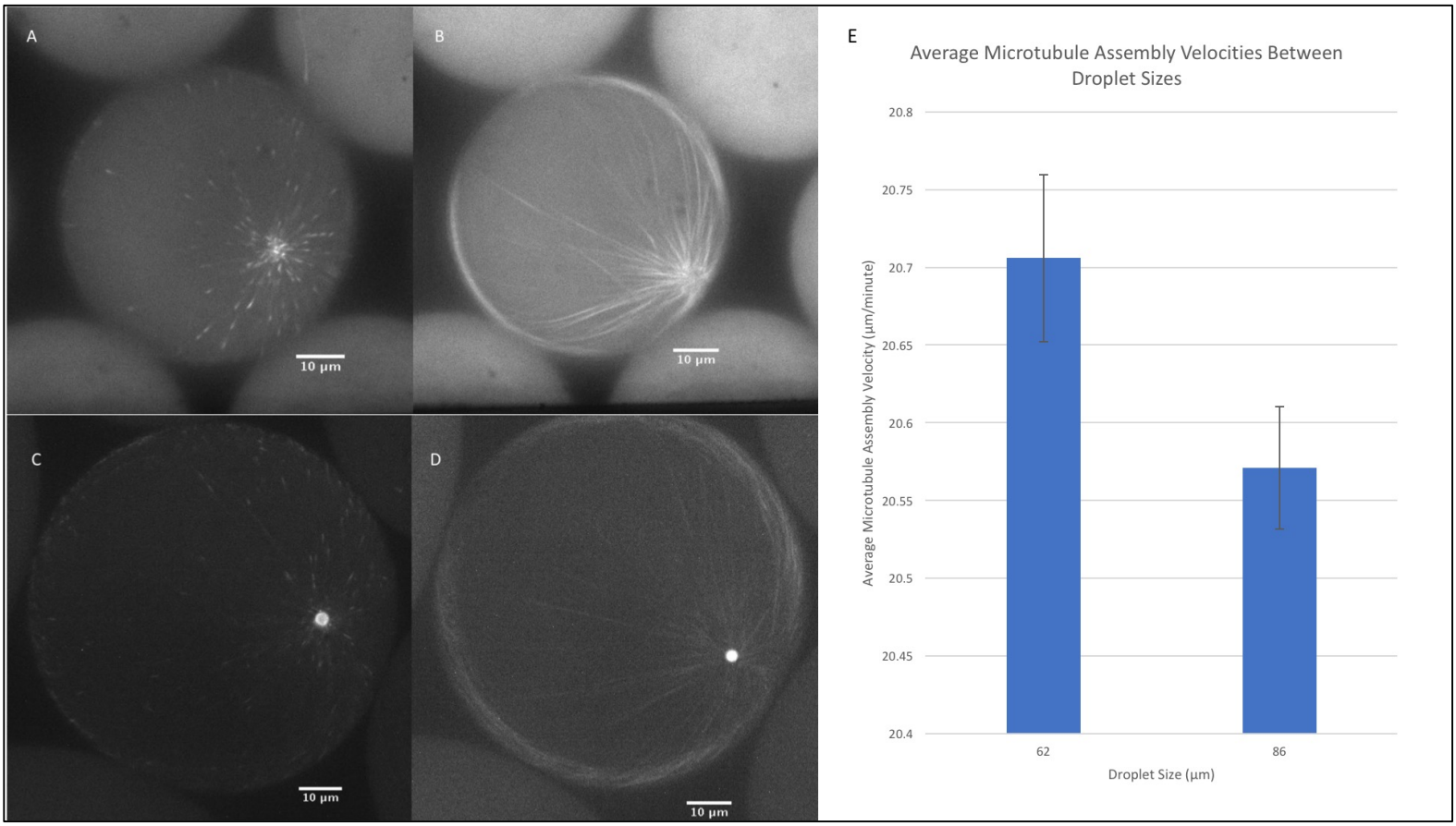

Figure 2: **A-B** single images obtained via confocal microscopy of EB1 and tubulin of the 62 µm droplet, respectively. **C-D** single images obtained via confocal microscopy of EB1 and tubulin of the 86 µm droplet, respectively. **E** the average velocities of the microtubule assembly between the two droplet sizes.

size. The 62µm droplet had an average microtubule assembly velocity of 20.706µm/minute, with a standard deviation of 0.0537. The 86 µm droplet had an average microtubule assembly velocitiy of 20.571µm/minute, with a standard deviation of 0.0396 (**Tables A-B**)**.** A two-tailed t-test reported the value of 0.9 suggests that there is no statistical difference between the average microtuble assembly velocity of these two droplets.

A

62µm diameter Droplet Microtubule Assembly Velocities		
Min Velocity (µm/sec)	Max Velocity (µm/sec)	Average Velocity (µm/sec)
0.257	0.506	0.383
0.293	0.586	0.431
0.311	0.605	0.42
0.262	0.568	0.383
0.364	0.38	0.37
0.313	0.537	0.392
0.154	0.517	0.259
0.154	0.438	0.309
0.154	0.325	0.26
0.131	0.364	0.25
0.182	0.524	0.308
0.257	0.402	0.331
0.154	0.474	0.345
0.073	0.505	0.406
0.185	0.402	0.308
0.154	0.444	0.357
0.284	0.488	0.359
0.255	0.438	0.331
0.131	0.392	0.306
0.284	0.575	0.394
Mean Velocity (µm/sec)		0.3451
Mean Velocity (µm/min)		20.706
Standard Deviation		0.053703768

B

86µm diameter Droplet Microtubule Assembly Velocities		
Min Velocity (µm/sec)	Max Velocity (µm/sec)	Average Velocity (µm/sec)
0.242	0.325	0.285
0.217	0.434	0.327
0.242	0.485	0.336
0.274	0.417	0.315
0.2	0.46	0.31
0.153	0.477	0.309
0.291	0.414	0.348
0.247	0.4	0.317
0.175	0.379	0.293
0.247	0.46	0.373
0.307	0.46	0.359
0.175	0.567	0.401
0.261	0.542	0.403
0.247	0.46	0.367
0.175	0.436	0.337
0.343	0.417	0.379
0.261	0.457	0.381
0.175	0.343	0.266
0.339	0.447	0.388
0.291	0.542	0.363
Mean Velocity (µm/sec)		0.34285
Mean Velocity (µm/min)		20.571
Standard Deviation		0.039553129

Tables **A-B**: Minimum, maximum, and average velocities of 20 different tracked EB1 comets for the 62µm and 86µm droplets.

Discussion:

We sought to determine the effect cell size has on the rate of microtubule assembly. As discussed, the limiting component model suggests that smaller cells would assemble microtubules at a slower rate than larger cells. The absolute concentration of enzymes and tubulin required for microtubule growth would depleted faster in a droplet with a smaller volume than a droplet with a large volume. A large cell would have a large cytoplasm with more volume than a small cell. When microtubules are constructed in the cell, this means that there would be more enzymes and resources within the cytoplasm that are readily available compared to cells of a smaller volume. When experimenting, we worked to test this model while operating under a couple assumptions that were not assessed. First, we believed that each sized droplet would have the same relative initial concentration of building blocks, especially XMAP215, required for microtubule assembly. Secondly, we assumed that the number of growing microtubule ends would be the same for each system, i.e. that this parameter would not scale with cytoplasmic volume. This means that the same number of XMAP215 molecules that were being drawn out of solution to facilitate microtubule assembly would be the same for each growing microtubule end despite droplet size. As previously stated, each molecule XMAP215 can add 25 tubulin dimers to the growing end of the microtubules per binding event (Brouhard et al, 2008), which we assumed was true of each droplet size.

We expected the average microtubule assembly velocity of the smaller droplet to be slower than the larger droplet. The results of this experiment are not what we predicted. This provides us information on where to take the experiments in the future. It is possible that the difference in

size between the two droplets in this experiment was not substantial enough to make a statistical difference in microtubule assembly velocity. Previous research has suggested the maximum velocity of growth of a microtubule, such that occurs when all possible XMAP215 binding sites at the growing end our occupied, is between 20-25µm/minute This is close to what was observed in both droplet sizes explored in these studies. This might suggest that all microtubule ends are saturated even in the smaller droplet, however, this is inconsistent with previous results from the Gatlin lab (unpublished data). Additionally, we would expect more growing ends to be produced by a spindle relative to a single aMTOC. This would impact the number of XMAP215 pulled from solution and whether each growing end is fully saturated with XMAP215 molecules. This could explain discrepancies with published spindle scaling data which show that spindles begin to scale with cell size when diameters are less than ~150 um (Good et al, 2013; Hazel et al, 2013). Future experiments could not only test smaller and larger droplet sizes than the ones used for this experiment, but also increase the number of droplets analyzed for this relationship.

References

A high-energy-density sugar biobattery based on a synthetic enzymatic pathway. Zhu, Z., Tam, T.K., Sun, F., You, C., Zhang, Y. H. P. (2014) Nature Communications. 3026.

Aneuploidy and tumorigenesis. Fang, X., Zhang, P. (2011). Seminars in Cell and Developmental Biology. 22(6): 595-601

Aqueous cigarette smoke extract induces a voltage-dependent inhibition of CFTR expressed in Xenopus oocytes. Moran, A.R., Norimatsu, Y., Dawson, D.C., MacDonald, K.D. (2014) American Journal of Physiology Lung Cell Molecular Physiology. 306(3) 284-291.

Aurora A kinase-coated beads function as microtubule-organizing centers and enhance RanGTP-induced spindle assembly. Tsai, M. Y., Zheng, Y. (2005) Current Biology. 15(23): 2156-2163

Changes in Cytoplasmic Volume are Sufficient to Drive Spindle Scaling. Hazel, J., Krutkramelis, K., Mooney, P., Tomschik, M., Gerow, K., Oakey, J., Gatlin, J.C. (2013). Science. 342(6160): 853-856.

Control of microtubule organization and dynamics: two ends in the limelight. Akhmanova, A., Steinmetz, M. O. (2015). Nature Reviews Molecular Cell Biology. 16(12): 711-726

Cytoplasmic volume modulates spindle size during embryogenesis. Good, M. C., Vahey, M. D., Skandarajah, A., Fletcher, D. A., Heald, R. (2013). Science. 343(6160): 856-860

Droplet microfluidics: A tool for biology, chemistry and nanotechnology. Mashaghi, S., Abbaspourrad, A., Weitz, D., van Oijen, A., M. (2016). Trends in Analytical Chemistry. 82: 118-125.

Evidence for an upper limit to mitotic spindle length. Wühr, M., Chen, Y., Dumont, S., Groen, A. C., Needleman, D. J., Salic, A., Mitchison, T. J. (2008). Current Biology. 18(16): 1256-1261

Force and length in the mitotic spindle. Dumont, S., Mitchison, T.J. (2009). Current Biology. 19(17): R749-761

Growth, interaction and positioning of microtubule asters in extremely large vertebrate embryo cells. Mitchison, T.J., Wühr, M., Nguyen, P., Ishihara, K., Groen, A., Field, C. M. (2012). Cytoskeleton. 69(10): 738-750

Heterogeneity of tubulin subunits. Feit, H., Slusarek, L., Shelanski, M. L. (1971). Proceedings of the National Academy of Sciences. 68(9): 2028-2031

High-Yield Production of Dihydrogen from Xylose by Using a Synthetic Enzyme Cascade in a Cell-Free System. Martín del Campo, J.S., Rollin, J., Myung, S., Chun, Y., Chandrayan, S., Patiño, R., Adams, M. W. W., Zhang, Y., H., P. Angwandte Chemie. 52(17): 4587-4590.

Induction of nuclear envelope breakdown, chromosome condensation, and spindle formation in cell-free extracts. Lohka, M. J., Maller, J. L. (1985) JCB. 101(2): 518.

Mechanisms of mitotic spindle assembly. Petry, S. Annual Review of Biochemistry. 85: 659-683

Studying DNA replication fork stability in Xenopus egg extract. Hashimoto, Y., Costanzo, V. (2011). Methods in Molecular Biology. 745: 437-445.

Tau co-organizes dynamic microtubule and actin networks. Elie, A., Prezel, E., Guérin, C., Denarier, E., Ramirez-Rios, S., Serre, L., Andrieux, A., Fourest-Lieuvin, A., Blanchoin, L., Arnal, I. (2015). Scientific Reports. 5: 9964

The use of Xenopus egg extracts to study mitotic spindle assembly and function in vitro. Desai, A., Murray, A., Michison, T. J., Walczak, C. E. (1999) Methods in Cell Biology. 61: 385-412.

Xenopus extract approaches to studying microtubule organization and signaling in cytokinesis. Field, C. M., Pelletier, J. F., Mitchison, T. J. (2017). Methods in Cell Biology. 137: 395-435

XMAP215 is a processive microtubule polymerase. Brouhard, G.J., Stear, J.H., Noetzel, T.L., Al-Bassam, J., Kinoshita, K., Harrison, C. H., Howard, J., Hyman, A. A. (2008) Cell. 132(1): 79-88.